ELSEVIER

www.elsevier.nl/locate/jorganchem

Journal of Organometallic Chemistry 598 (2000) 28–35

Journal of Organometallic Chemistry

Reactions of metalloalkynes☆ Part 6. Synthesis of open tetrametallic clusters. Reaction of [Ru(CO)$_4$(ethene)] with ethyne-1,2-diyl compounds. Single crystal X-ray structural determinations of [Ru$_4$(μ_4-CC)(η-C$_5$H$_4$R)$_2$(μ-CO)$_2$(CO)$_8$] (R = H, Me)

Lindsay T. Byrne, James P. Hos, George A. Koutsantonis *, Brian W. Skelton, Allan H. White

Department of Chemistry, University of Western Australia, Nedlands 6907, Perth, WA, Australia

Received 3 September 1999; received in revised form 19 October 1999

Abstract

The reactions between [Ru(CO)$_4$(η^2-C$_2$H$_4$)], generated in situ, and ruthenium ethyne-1,2-diyl complexes, [{Ru(CO)$_2$(η-C$_5$H$_4$R)}$_2$(μ-C≡C)] (R = H, Me) have provided the new air-sensitive complexes [Ru$_4$(μ_4-CC)(η-C$_5$H$_4$R)$_2$(μ-CO)$_2$(CO)$_8$] (R = H, Me) with a permetallated ethene structure, in good yield. The complexes were characterized spectroscopically and by single-crystal X-ray diffraction studies. They have an almost planar open geometry, rendering the C_2^{2-} ligand accessible to reaction. The resonances attributed to the C_2^{2-} ligand in the $^{13}C\{^1H\}$-NMR spectra of the complexes have been unequivocally assigned with the aid of labeling experiments. © 2000 Elsevier Science S.A. All rights reserved.

Keywords: Ruthenium; Cluster; Carbide; Tetranuclear

1. Introduction

Recent reports have examined the chemistry of ethyne-1,2-diyl compounds in an effort to rationally build well-defined metal aggregates [1–6]. The scope of established methods to develop medium to high nuclearity clusters is relatively well established [7,8] as is the incorporation of alkyne derived fragments [9,10]. However, a rational approach to sequential cluster expansion is lacking. In an earlier paper [2] we reported the synthesis of the pentanuclear cluster [Ru$_5$(μ_5-C≡C)(η-C$_5$H$_4$R)$_2$(dppm)(μ_2-CO)$_2$(CO)$_7$] using an ethyne-1,2-diyl template synthesis. This pentanuclear compound has proved unsuitable for further reactivity studies and we are seeking more reactive complexes to investigate catalytically important reactions. In this paper we report the reaction of [{Ru(CO)$_2$(η-C$_5$H$_4$R)}$_2$(μ-C≡C)] (**1a**, R = H; **1b**, R = Me) with reactive ruthenium carbonyl equivalents, [Ru(CO)$_4$(η^2-C$_2$H$_4$)].

2. Results and discussion

The ethylene substituted complex [Ru(η^2-C$_2$H$_4$)(CO)$_4$] (**2**) [11], is a convenient source of lightly stabilized Ru(CO)$_4$ units [12] and the stoichiometric reaction between this and **1** gave a red solution immediately. The presence of residual **1** was evident (TLC, IR), attempts to separate the red product being thwarted by its rapid decomposition in air. In a similar reaction, two equivalents of **2** with one equivalent of **1a** or **1b** (Scheme 1) proceeded similarly, complete consumption of complex **1** being observed. Crystallization under an inert atmosphere, directly from the reaction mixture, yielded dark-red crystals of the tetranuclear cluster, structurally characterized as [Ru$_4$(μ_4-CC)(η-C$_5$H$_4$R)$_2$(μ-

☆ Ref. [1] is regarded as Part 5.

* Corresponding author. Fax: +61-9-380-1005.

E-mail address: gak@chem.uwa.edu.au (G.A. Koutsantonis)

0022-328X/00/$ - see front matter © 2000 Elsevier Science S.A. All rights reserved.
PII: S0022-328X(99)00666-X

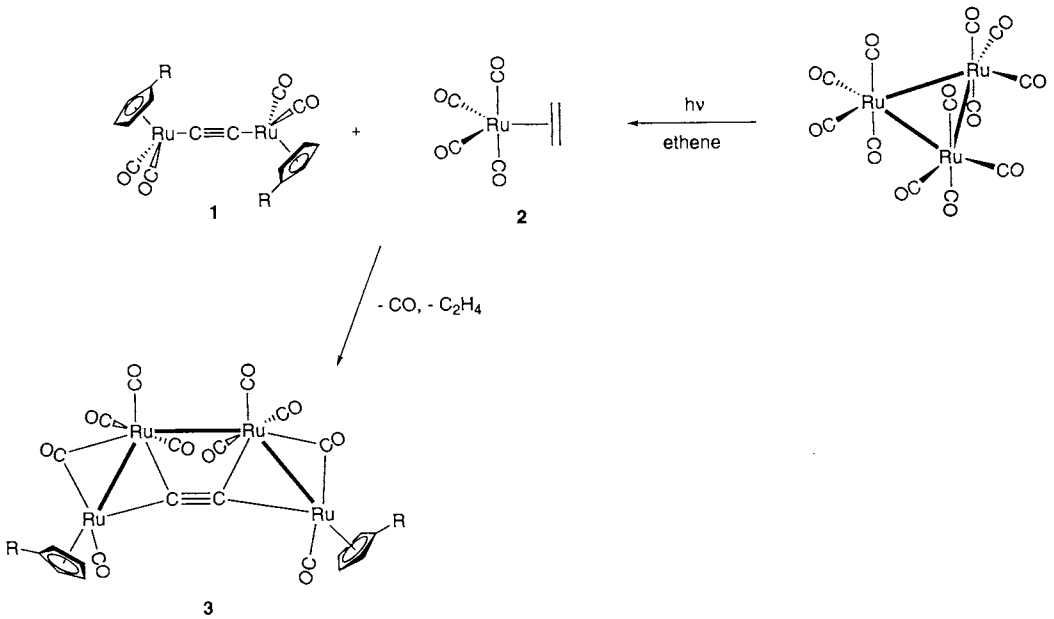

Scheme 1. **a**, R = H; **b**, R = Me.

$CO)_2(CO)_8$] (**3a**, R = H; **3b**, R = Me). Whilst only moderate yields of the complexes **3** were recovered (50–60%), the IR and NMR spectra of the reaction mixtures were consistent with their quantitative formation.

The carbonyl stretching bands observed in the solution IR spectra confirmed the existence of both terminal and bridging carbonyl ligands. The ^{1}H-NMR spectra showed resonances indicative of two equivalent (η^5-C_5H_4R) groups per molecule. The ^{1}H-NMR spectra of complex **3a** contains a single resonance for the ten (η^5-C_5H_5) protons at 4.66 ppm, whilst **3b** has a resonance at 1.32 ppm for the six methyl protons with four signals for the two sets of equivalent CH protons. The FAB MS of both complexes have molecular ions and fragmentation consistent with the loss of carbonyl ligands. The spectrum of complex **3a** shows the loss of six molecules of CO, whilst **3b** yields daughter ions for the loss of up to ten CO ligands.

2.1. Solid-state structure of complexes *3a* and *3b*

The results of the room temperature structure determinations on specimens obtained from CH_2Cl_2–hexanes are presented in Figs. 1 and 2, with relevant interatomic parameters in Table 1. Details of the structure solution and refinement are contained in Table 2.

The results of the room temperature single-crystal X-ray structure determinations are consistent with the stoichiometries and connectivities implied by the above formulations **3a**, **3b**, one and two molecules respectively (**3a** accompanied by a dichloromethane of solvation), devoid of crystallographic symmetry, comprising the asymmetric units of their structures. Both complexes comprise, within each molecule, pairs of [{(η^5-C_5H_4R)$(CO)_5Ru_2$)}C] moieties linked by bonds between the pairs of carbide atoms and pairs of (one of) the two ruthenium atoms, the overall aggregate comprising a quasi-planar array made up of the four ruthenium atoms, the carbide moiety disposed between them, and at each periphery one of the carbonyl groups (CO(12)) bridging its two associated ruthenium atoms: the other moieties are disposed to either side of the plane (Fig. 3).

The planar arrangement of four metal moieties about a dicarbon unit has previously been described structurally in the complex [$Fe_2Ru_2(\mu_4$-CC)$(CO)_8(\mu$-$CO)_2(\eta$-$C_5Me_5)$] as a 'permetallated ethene' [13,14]; the present **3a**, **3b** are further examples of this rare tetranuclear geometry [15].

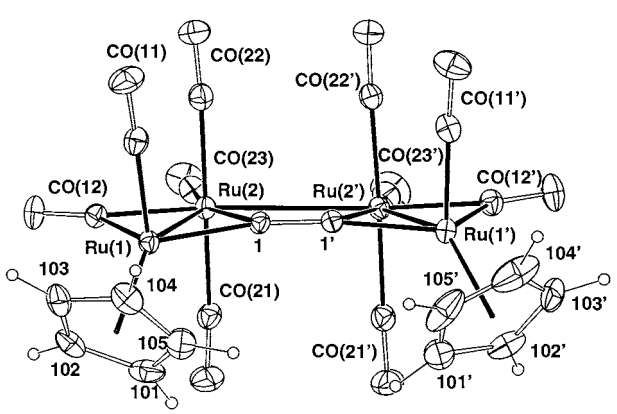

Fig. 1. Molecular projection of complex **3a**, almost through the $Ru_4C_2(CO)_2$ core plane. 20% Probability ellipsoids are shown for the non-hydrogen atoms; hydrogen atoms having arbitrary radii of 0.1 Å.

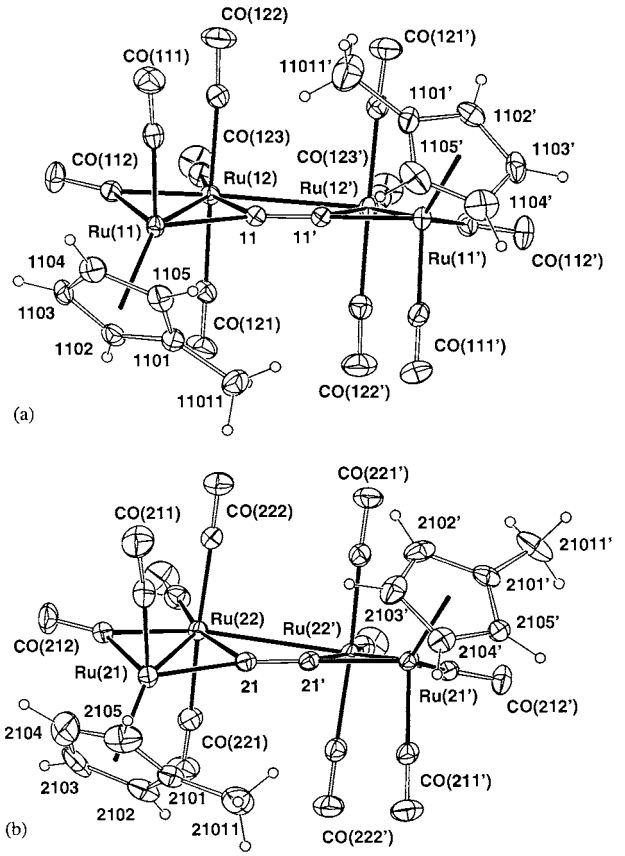

Fig. 2. (a), (b) Molecular projections of complex **3b** (two molecules).

Within the present Ru_4 plane, the Ru(2)···Ru(2′) interaction is long (Table 2), presumably a weaker link between the two halves of the molecule than the C(1)–C(1′) interactions, which are of a length characteristic of a bond order mid-way between double and triple. The bridging carbonyl groups are equably disposed between their two associated ruthenium atoms; in **3b**, the associated Ru(1,2)–C(12) distances are only trivially different, but in **3a**, the difference is consistently ca 0.06 Å, Ru(1)–C(12) being consistently longer. The associated angles Ru(1,2)–C(12)–O(12) show similar behavior, with trivial differences in **3b** but with the Ru(2)–C(12)–O(12) slightly greater than Ru(1)–C(12)–O(12) in **3a**. Among the C–O distances of the carbonyl groups, those associated with CO(12) are slightly but consistently lengthened vis-à-vis the remainder in keeping with its bridging rather than terminal bonding mode. In **3a**, the Ru_4C_2 core is more closely planar ($\chi^2 = 6578$; atom deviations δ Ru (1,1′, 2,2′), C(1,1′) −0.035(1), 0.019(1), 0.044(1), −0.048(1), 0.146(4), 0.139(4) Å) than in **3b**, (molecule 1: χ^2 3×10^4; δ (same order) 0.077(1), −0.073(1), −0.127(1), 0.127(1), −0.030(3), −0.014(3) Å); molecule 2: χ^2 1×10^6; δ 0.140(1), −0.139(1), −0.238(1), 0.242(1), 0.026(3), −0.037(3) Å), the distortion in **3a** corresponding to a slight bowing to either side of the putative mirror plane normal to the Ru_2C_2 array, while in **3b**, the distortion takes the form of a twist about the putative 2-axis which lies within the Ru_2C_2 'plane'.

These two types of distortion are in keeping with the putative symmetries within each of the aggregate types found within the molecules of each of the two compounds. The parent [{(η^5-C_5H_4R)$(OC)_5Ru_2$}C] moiety, with the η^5-C_5H_4R moiety bound to one side of the plane is inherently chiral, and the coupling of pairs of moieties by plane formation of the above type can be effected by combining the pair as mirror images, to form a species with putative internal *m*-symmetry, a *syn-/cisoid* array, as in **3a**, or by combining pairs of similar chirality to form an array with putative 2-symmetry, an *anti-/transoid* array, as in **3b** (Fig. 1). Individual molecules of the latter are, of course, chiral, but the overall array within the crystal, conforming to the symmetry of a centrosymmetric space group, is also a racemate. In **3b**, the two molecules which comprise the asymmetric unit are not pseudo-symmetrically related, displaying distinct differences in respect of the relative dispositions of their cyclopentadienide methyl substituents. Despite the differences in distortions within the plane noted above, the geometries of the individual hemimolecular components (Table 2) display only trivial systematic differences across the various combinations of isomeric and substituent possibilities encompassed here. Of more interest are the global variations within these moieties. We find Ru(1)–C(11) to be appreciably shorter than the other ruthenium–terminal carbonyl–carbon distances, although Ru(2)–C(23) also approaches that lower limit, in keeping with the lengthening of Ru(2)–C(1) cf. Ru(1)–C(1). The latter feature, together with the long Ru (2)···Ru(2′) distances, is in accord with related findings [13,14], all four ruthenium centers exhibiting 18 valence electron counts. The (substituted) cyclopentadienide ligands are unsymmetrically coordinated, Ru–C ranging over up to 0.1 Å; the more diverse ranges are found in **3b**, the smallest value, typically ca. 2.20 Å, consistently being found at C(n04), suggesting that the presence of the substituent does influence these distances slightly but significantly; although not interacting with the ambience so that one particular orientation is dictated, nevertheless, three of the four substituents have a similar orientation which would result in mutual fouling in an array of *m*- rather than 2-symmetry, and this may have some bearing on the nature of the associated isomer.

2.2. ^{13}C-NMR investigation of isotopically enriched *3a*

The assignment of NMR signals arising from the presence of carbonyl and carbide ligands is often difficult as in general they are of a low intensity. One strategy for assignment is via the isotopic enrichment of the complexes using either ^{13}C carbon monoxide or ^{13}C

Table 1
Molecular non-hydrogen geometries (bond lengths (Å) and bond angles (°)) for **3a** and **3b** [a]

Atoms	**3a**	**3b** (molecule 1)	**3b** (molecule 2)
Bond angles			
Ru(1)–Ru(2)	2.7988(4), 2.7873(5)	2.8023(4), 2.8030(4)	2.8060(4), 2.7992(4)
Ru(2)···Ru(2′)	3.0190(5)	3.0423(3)	3.0366(4)
Ru(1)–C(1)	2.030(3), 2.030(4)	2.015(3), 2.021(3)	2.023(3), 2.021(3)
Ru(2)–C(1)	2.240(4), 2.225(3)	2.207(3), 2.212(3)	2.241(3), 2.211(3)
C(1)–C(1′)	1.258(5)	1.258(4)	1.252(4)
Ru(1)–C(11)	1.866(4), 1.858(5)	1.862(4), 1.866(4)	1.846(5), 1.852(4)
Ru(1)–C(12)	2.104(5), 2.098(4)	2.065(4), 2.064(5)	2.057(3), 2.073(4)
Ru(2)–C(12)	2.043(4), 2.040 (5)	2.059(3), 2.056(3)	2.054(3), 2.054(3)
Ru(2)–C(21)	1.943(4), 1.934(5)	1.937(7), 1.959(3)	1.935(4), 1.915(4)
Ru(2)–C(22)	1.956(4), 1.961(4)	1.932(4), 1.943(4)	1.948(4), 1.947(4)
Ru(2)–C(23)	1.885(5), 1.890(5)	1.883(4), 1.887(4)	1.883(4), 1.882(4)
Ru(1)–C(10n)	2.242(4)–2.260(6)	2.200(4)–2.307(3)	2.186(6)–2.288(4)
Ru(1′)–C(10n′)	2.21(1)–2.257(6)	2.208(5)–2.279(4)	2.201(4)–2.298(4)
<Ru(1)–C(10n)>	2.25, 2.23	2.25, 2.25	2.24, 2.25
Ru(1)–C(100)	1.905, 1.900	1.902, 1.907	1.895, 1.899
C(11)–O(11)	1.139(6), 1.153(6)	1.146(5), 1.130(4)	1.148(6), 1.150(5)
C(12)–O(12)	1.164(6), 1.164(5)	1.174(4), 1.170(4)	1.169(4), 1.168(4)
C(21)–O(21)	1.121(6), 1.133(6)	1.129(4), 1.122(4)	1.129(6), 1.131(5)
C(22)–O(22)	1.132(5), 1.118(5)	1.134(5), 1.134(5)	1.128(5), 1.133(5)
C(23)–O(23)	1.144(6), 1.137(6)	1.143(5), 1.141(5)	1.148(5), 1.148(5)
Bond angles			
Ru(1)–Ru(2)–Ru(2′)	111.38(2), 113.68(1)	111.91(1), 111.04(1)	109.58(1), 112.24(1)
C(100)–Ru(1)–C(1)	123.5, 124.3	122.7, 122.9	122.9 123.7
C(100)–Ru(1)–Ru(2)	136.7, 134.2	135.0, 137.0	135.7, 135.3
C(100)–Ru(1)–C(11)	126.4, 128.2	127.9, 126.5	127.0, 126.4
C(100)–Ru(1)–C(12)	118.2, 116.6	119.6, 120.6	120.2, 119.6
C(1)–Ru(1)–Ru(2)	52.4(1), 52.17(9)	51.41(9), 51.52(9)	52.30(8), 51.52(9)
C(1)–Ru(1)–C(11)	91.8(2), 90.6(2)	91.1(1), 89.4(1)	91.4(2), 90.2(1)
C(1)–Ru(1)–C(12)	98.7(2), 98.4(2)	97.9(1), 98.0(1)	98.4(1), 97.7(1)
Ru(2)–Ru(1)–C(11)	96.4(1), 96.9(2)	96.8(1), 96.3(1)	96.9(1), 98.0(1)
Ru(2)–Ru(1)–C(12)	46.65(9), 46.8(1)	47.11(9), 47.01(9)	46.9(1), 47.01(9)
C(12)–Ru(1)–C(11)	90.2(2), 90.4(2)	89.2(2), 90.9(1)	88.2(2), 90.5(1)
Ru(1)–C(11)–O(11)	176.7(4), 176.0(5)	177.2(3), 177.5(4)	176.3(3), 176.6(3)
Ru(1)–C(12)–O(12)	136.3(3), 135.3(4)	136.6(3), 137.1(3)	136.6(3), 136.8(3)
Ru(2)–C(12)–O(12)	138.7(3), 140.0(4)	137.8(3), 137.1(3)	137.2(3), 137.7(3)
Ru(1)–C(12)–Ru(2)	84.9(2), 84.7(1)	85.6(1), 85.7(1)	86.1(1), 85.4(1)
Ru(1)–C(1)–Ru(2)	81.8(2), 81.7(1)	83.0(1), 82.8(1)	82.1(1), 82.7(1)
Ru(1)–C(1)–C(1′)	162.5(3), 165.9(3)	164.1(3), 162.3(3)	163.3(2), 165.6(3)
C(1′)–C(1)–Ru(2)	114.7(3), 111.8(3)	112.5(2), 114.9(2)	114.4(2), 111.7(2)
C(1)–Ru(2)–C(12)	94.0(2), 94.1(2)	92.2(1), 92.4(1)	91.8(1), 92.5(1)
C(1)–Ru(2)–Ru(1)	45.88(8), 46.1(21)	45.55(7), 45.68(8)	45.57(8), 45.73(8)
C(1)–Ru(2)–C(21)	93.9(2), 90.9(2)	93.7(1), 93.2(1)	97.5(1), 93.8(1)
C(1)–Ru(2)–C(22)	89.5(2), 88.4(1)	89.5(1), 89.6(1)	85.4(1), 87.1(1)
C(1)–Ru(2)–C(23)	161.9(2), 162.1(2)	162.5(1), 162.3(1)	167.4(1), 166.0(1)
C(1)–Ru(2)–Ru(2′)	65.89(9), 67.6(1)	66.71(7), 65.56(8)	65.03(8), 67.23(8)
C(12)–Ru(2)–Ru(1)	48.5(1), 48.5(1)	47.3(1), 47.3(1)	46.99(9), 47.6(1)
C(12)–Ru(2)–C(21)	91.7(2), 93.5(2)	94.1(1), 92.3(1)	93.8(2), 93.2(1)
C(12)–Ru(2)–C(22)	88.7(2), 88.9(2)	88.6(1), 88.0(1)	91.6(1), 90.2(1)
C(12)–Ru(2)–C(23)	103.9(2), 103.7(2)	105.2(1), 105.3(1)	100.0(1), 101.3(1)
C(12)–Ru(2)–Ru(2′)	159.9(1), 161.1(1)	158.9(1), 157.9(1)	156.57(9), 159.72(9)
Ru(1)–Ru(2)–C(21)	89.6(1), 87.5(2)	89.6(1), 88.4(1)	91.7(1), 88.3(1)
Ru(1)–Ru(2)–C(22)	93.2(1), 93.7(1)	94.6(1), 93.9(1)	94.2(1), 94.9(1)
Ru(1)–Ru(2)–C(23)	152.2(1), 151.7(2)	152.0(1), 152.0(1)	146.7(1), 148.3(1)
Ru(1)–Ru(2)–Ru(2′)	111.38(2), 113.68(1)	111.91(1), 111.04(1)	109.58(1), 112.24(1)
C(21)–Ru(2)–C(22)	176.6(2), 177.5(2)	175.8(2), 177.2(2)	173.8(1), 176.4(1)
C(21)–Ru(2)–C(23)	87.5(2), 89.4(2)	87.4(2), 87.2(2)	86.0(2), 87.9(2)
C(22)–Ru(2)–C(23)	89.1(2), 90.5(2)	88.8(2), 90.0(2)	90.1(2), 90.3(2)
C(21)–Ru(2)–Ru(2′)	88.3(1), 91.7(1)	88.39(9), 90.86(9)	86.0(2), 87.3(2)
C(22)–Ru(2)–Ru(2′)	92.4(1), 85.9(1)	90.2(1), 89.8(1)	90.3(1), 89.9(1)
C(23)–Ru(2)–Ru(2′)	96.2(1), 94.5(2)	95.8(1), 96.7(1)	103.4(1), 99.0(1)
Ru(2)–C(21)–O(21)	176.2(4), 177.8(4)	177.2(3), 176.3(3)	174.7(3), 176.9(3)
Ru(2)–C(22)–O(22)	177.1(5), 177.6(4)	177.1(3), 176.8(3)	178.9(3), 178.7(3)
Ru(2)–C(23)–O(23)	179.1(4), 178.0(4)	178.8(3), 178.2(3)	176.9(3), 178.2(3)

[a] Within each molecule values are given for the unprimed, primed sections, respectively; C(100) is the cp centroid.

Table 2
Summary of diffraction data for complexes **3**

	3a	**3b**
Formula	$C_{23}H_{12}Cl_2O_{10}Ru_4$	$C_{24}H_{14}O_{10}Ru_4$
M_r	923.53	866.65
Crystal system	Monoclinic	Triclinic
Space group	$P2_1/c$	$P\bar{1}$
a (Å)	14.613(1)	9.0101(4)
b (Å)	12.949(1)	15.8355(8)
c (Å)	16.400(2)	19.1107(9)
α (°)	90.0	89.711(1)
β (°)	115.804(1)	86.295(1)
γ (°)	90.0	78.741(1)
U (Å^3)	2793.8(4)	2668.6(8)
Z	4	4
μ_{Mo} (cm^{-1})	23.6	22.7
Specimen size (mm)	$0.52 \times 0.23 \times 0.23$	$0.31 \times 0.27 \times 2.20$
$T^*_{min/max}$	0.607/0.837	0.460/0.647
$2\theta_{max}$ (°)	58	58
N_{total}	31635	29261
N (R_{int})	7051 (0.034)	12 971 (0.024)
N_o	5797	10 966
R	0.032	0.027
R'	0.043	0.020

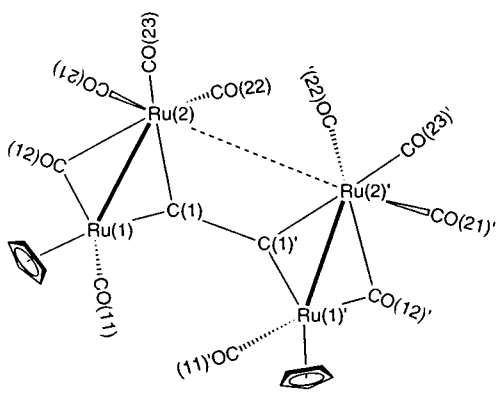

Fig. 3. Diagram showing labeling scheme used in complexes **3** for discussion of structural and NMR data.

enrichment of the C(sp) of the ethyne-1,2-diyl ligand, where recent successes in assigning carbide signals using the former process [1] have resulted.

The complex [^{13}CO]-**3a** was prepared using ^{13}CO enriched [$Ru_3(CO)_{12}$], (whence [^{13}CO]-**2**), allowing assignment of the single resonance at 154.9 ppm in the $^{13}C\{^1H\}$-NMR spectrum of [^{13}CO]-**3a** as that of the carbido unit. The compound gives a spectrum consistent with the equivalence of cyclopentadienyl ligands and the existence of a (pseudo) mirror plane, which allows assignment of the five enhanced resonances to carbonyl ligands. The spectrum also clearly shows the existence of a second sequence of resonances for the six signals in the region 160–240 ppm. The series of smaller peaks offset slightly from the larger ones, at about 15% of the dominant intensity, are proposed to arise from the existence of two isomers of **3a**, generated during the formation of the complex (see below Scheme 2). One possible explanation for this observation is the isomerism described above; the major species is presumably containing (η-C_5H_5) ligands in the *synclinal* configuration, as isolated and structurally characterized, with the minor isomer featuring the ligands in a presumably *anticlinal* orientation.

The ^{13}C enrichment of the carbonyl ligands has allowed the observation of ^{13}C–^{13}C coupling on four of the five carbonyl resonances. The most downfield singlet is assigned to the bridging carbonyl and is uncoupled. The shape of the coupled signals appear ostensibly as triplets, but this appears unlikely as no ABB′ spin systems exist and the peak integrals are far from the required 1:3:1. We presumably observe ^{13}C–^{13}C coupling only in those molecules that have sufficiently enriched carbonyls, as the enrichment may not be necessarily uniform on each ruthenium atom throughout the sample. We therefore should see isotopically enhanced singlets for the remaining molecules, overlaid with the doublet arising from coupling of enriched carbonyls. We can assign the carbonyl resonances with the aid of the solid state structure, simplified for this procedure below (Fig. 3), via the application of the Karplus relation [16]. Carbon nuclei C(21) and C(22) couple favorably with each other given the near linear C(21)–Ru(2)–C(22) angle of 175.8°, giving rise to resonances at 194.5 ppm ($^2J_{CC} = 39.0$ Hz) and 191.4 ppm ($^2J_{CC} = 39.0$ Hz). The bridging carbonyl C(12) is assigned to the downfield signal at 240.5 ppm and is uncoupled, presumably due to almost orthogonal dihedral angles relative to other nuclei. The singlet at 198.3 ppm is most likely to arise from C(23), since the bond to it lies effectively perpendicular to the C(21)–C(22) vector, with bond angles in the solid state of C(23)–Ru(2)–C(21), C(22) = 87.4, 88.8°. Atom C(23) also appears unfavorably placed to couple with either C(12) or C(11). The weakly coupled signal at 205.4 ppm is split with $J = 6.4$ Hz, presumably arising from C(11) coupling through three bonds to C(21) or C(22).

2.3. Formation of the complexes

The reaction of [{$Ru(CO)_2(\eta$-$C_5H_4R)$}$_2(\mu$-C≡C)] (**1a**, R = H; **1b**, R = Me) with [$Ru_3(CO)_{12}$], in refluxing toluene gave an intractable mixture of products. In the analogous reaction of [{$Fe(CO)_2(\eta$-$C_5Me_5)$}$_2(\mu$-C≡C)] with [$Ru_3(CO)_{12}$], a complex mixture of products resulted of which the analog of complexes **3** [$Fe_2Ru_2(\mu_4$-CC)$(CO)_8(\mu$-$CO)_2(\eta$-$C_5Me_5)$] was but a minor component [13,14]. In seeking more effective methods of increasing the selectivity of this type of reaction, one approach used the reaction of **1** with [$Ru_3(CO)_{10}$-$(NCMe)_2$], utilizing the easily substituted MeCN ligands to attain increased reactivity, in the manner well known for alkynes [7,17]. However, this was also un-

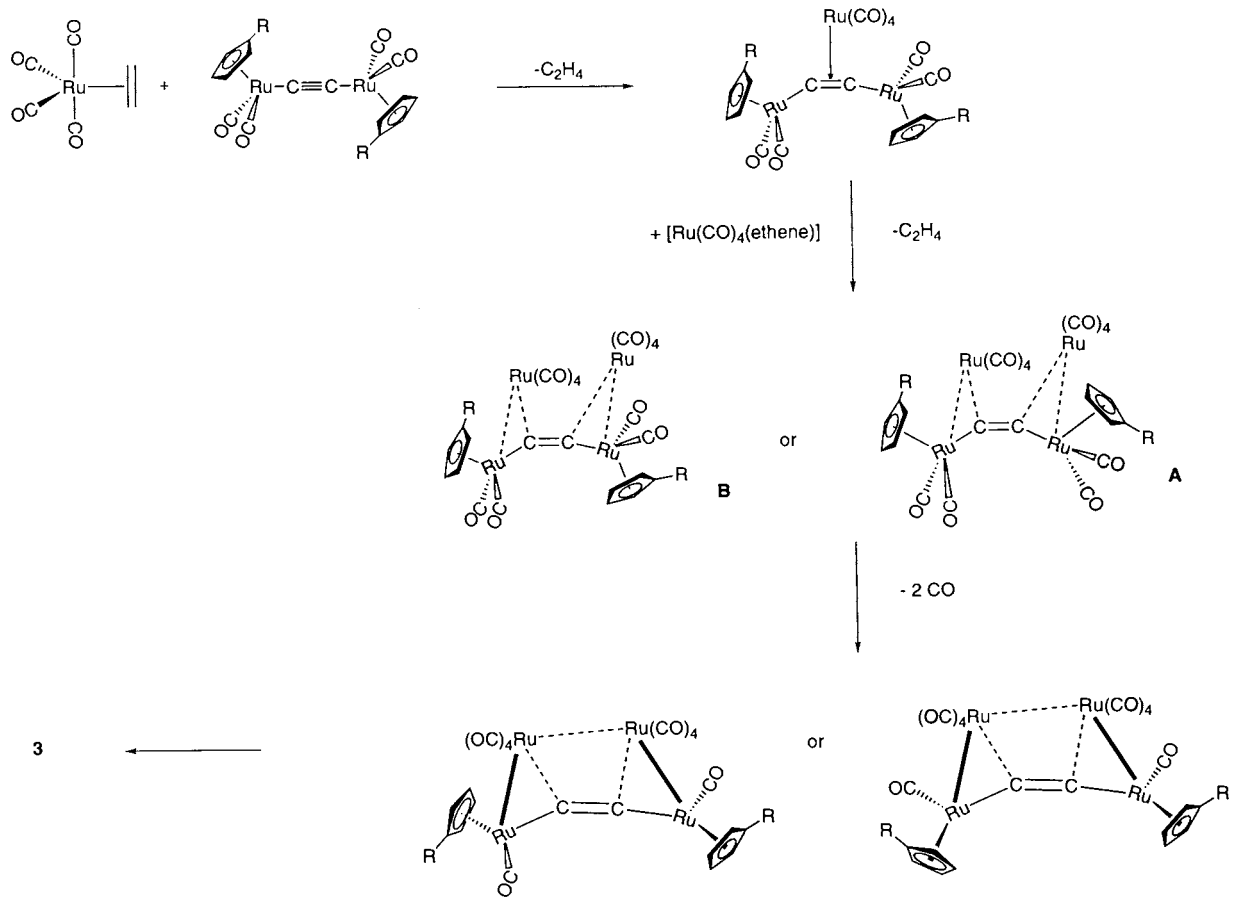

Scheme 2.

successful giving mixtures that were not amenable to chromatography.

At this point we turned to $[Ru(\eta^2\text{-}C_2H_4)(CO)_4]$ (**2**), produced in situ from the photochemical reaction of $[Ru_3(CO)_{12}]$ and ethene, which reacted readily and in a selective manner. The probable course of reaction between **1** and **2** (Scheme 2) involves the initial coordination of an $Ru(CO)_4$ group to the CC unit in an η^2-fashion, with concomitant loss of the weakly bound ethylene ligand. It is unclear at what point the metal–metal bonds are formed and whether this is preceded or not by the coordination of the second $Ru(CO)_4$ unit. The $Ru(CO)_2(C_5H_4R)$ units are free to rotate about the Ru–C(sp) bond and the initial coordination should cause the $Ru(CO)_2(C_5H_4R)$ unit to bend away from the incoming $Ru(CO)_4$ moiety, with the cyclopentadienyl ligand rotating. Presumably the steric requirements of the cyclopentadienyl ligands direct the formation of the metal–metal bonds in such a manner as to relieve any potential encumbrance. The observed difference in stereochemistry of **3a** and **3b** can possibly be accounted for thus in the formation of the complexes. Isomerism was only observed in the ^{1}H-NMR spectrum of **3a** which contains the less sterically demanding (η-C_5H_5) ligand and these isomers not being found to interconvert. One possible mechanism for interconversion of the final products could involve breaking of the long Ru–Ru bond with rotation about the 'ethene' carbon–carbon bond, but this is unlikely to result in a change of chirality and is a process that should be too high in energy. Thus, the isomers arise from the process of formation, in particular, at the second addition of a $Ru(CO)_4$ group, the degree of rotation and bending back of the Ru–C(sp) bonds being the determinant of the final stereochemical outcome (Scheme 2, **A** or **B**).

3. Conclusions

We have used a rational route to the synthesis of open, tetrametallic cluster complexes, $[Ru_4(\mu_4\text{-}CC)(\eta\text{-}C_5H_4R)_2(\mu\text{-}CO)_2(CO)_8]$ (**3a**, R = H; **3b**, R = Me) which we found to be unusually air-sensitive, once again demonstrating the templating ability of the ethyne-1,2-diyl ligand and its utility in the formation of multimetallic species.

4. Experimental

4.1. General conditions

Manipulation of oxygen and moisture sensitive compounds was performed under an atmosphere of high purity argon using standard Schlenk techniques or in a dry box (Miller Howe).

IR spectra were recorded using a Bio-Rad FTS 45 or 40 FTIR spectrometer. ^{1}H- and ^{13}C-NMR spectra were acquired using a Varian Gemini 200 or Bruker ARX 500 spectrometers. ^{31}P-NMR spectra were acquired using a Bruker ARX 500 spectrometer. ^{1}H- and ^{13}C-NMR spectra were referenced with respect to incompletely deuterated solvent signals.

Mass spectra were obtained on a VG AutoSpec spectrometer employing a fast atom bombardment (FAB) ionization source in all samples unless otherwise specified.

Elemental analysis were performed by the Research School of Chemistry Microanalytical Unit, Australian National University, ACT.

Tetrahydrofuran was dried over sodium metal and distilled from potassium benzophenone ketyl under an atmosphere of argon. *n*-Hexane and toluene were dried over sodium metal and distilled from sodium benzophenone ketyl under an atmosphere of argon. Distilled solvents were stored over sodium or potassium mirrors until use.

4.2. Preparation of $[Ru_4(\mu_4\text{-}CC)(\eta\text{-}C_5H_5)_2(\mu\text{-}CO)_2(CO)_8]$ (**3a**)

A solution of $\{Ru(CO)_2(\eta\text{-}C_5H_5)\}_2(\mu\text{-}C{\equiv}C)$ (**1a**) (50 mg, 0.107 mmol) in THF was added dropwise with stirring to a freshly prepared solution of $(\eta^2\text{-}C_2H_4)Ru(CO)_4$ (0.216 mmol) in *n*-hexane. Addition was accompanied by a fast color change (ca. 5 min) from light brown to red. The solvent was removed in vacuo and the mixture recrystallized (CH_2Cl_2–*n*-hexane) giving dark red crystals of **3a** (30 mg, 67%). Anal. Calc. for $C_{22}H_{10}O_{10}Ru_4$: C, 31.50; H, 1.20. Found: C, 31.52; H, 1.17%. IR (CH_2Cl_2) ν(CO) 2094 m, 2060 m, 2018 vs, 1997 s, 1972 s, 1797 s cm^{-1}. ^{1}H-NMR δ (C_6D_6) 4.66 (s, 10H, C_5H_5); ^{13}C{^{1}H}-NMR δ (C_6D_6) 89.7 (s, C_5H_5), 154.9 (s, *C*C), 191.2 (s, CO), 194.5 (s, CO), 198.3 (s, CO), 205.3 (s, CO), 240.3 (s, μ-CO). FAB MS (NOBA–CH_2Cl_2) *m*/*z* 840 ([M]$^+$, 46%), 812, 784, 756, 728, 700, 672 ([M − *n*CO]$^+$, *n* = 1–6, 90%, 88%, 100%, 66%, 45%, 45%).

4.3. Preparation of $[Ru_4(\mu_4\text{-}CC)(\eta\text{-}C_5H_4Me)_2(\mu\text{-}CO)_2(CO)_8]$ (**3b**)

In a manner similar to **3a**, $[(\eta^2\text{-}C_2H_4)Ru(CO)_4]$ (0.15 mmol) and **1b** (35 mg, 0.07 mmol) were reacted to yield **3b** (25 mg, 57%). Anal. Calc. for $C_{24}H_{14}O_{10}Ru_4$: C, 33.25; H, 1.63. Found: C, 32.53; H, 1.83%. IR (CH_2Cl_2) ν(CO) 2094 m, 2060 m, 2018 vs, 1997 s, 1972 s, 1797 s cm^{-1}. ^{1}H-NMR δ (C_6D_6) 1.66 (s, 6H, C_5H_4Me), 4.15 (m, 2H, C_5H_4Me), 4.63 (m, 2H, C_5H_4Me), 4.69 (m, 2H, C_5H_4Me), 4.92 (m, 2H, C_5H_4Me). ^{13}C{^{1}H}-NMR δ (C_6D_6) 13.2 (s, 2 × C_5H_4Me), 86.3 (s, C_5H_4Me), 87.4, 88.9 (s, C_5H_4Me), 91.3 (s, C_5H_4Me), 111.4 (s, C_i–C_5H_4Me), 157.1 (s, *C*C), 191.4 (s, CO), 194.4 (s, CO), 198.4 (s, CO), 205.3 (s, CO), 242.0 (s, μ-CO). FAB MS (NOBA–CH_2Cl_2) *m*/*z* 868 ([M]$^+$, 61%), 840, 812, 784, 756, 728, 700, 672, 644, 616, 588 ([M − *n*CO]$^+$, *n* = 1–10, 95%, 100%, 82%, 50%, 72%, 50%, 35%, 80%).

4.4. Crystallography

Full spheres of area-detector diffraction data were measured within the limit $2\theta_{max} = 58$ at ca. 300 K using a Bruker AXS CCD instrument fitted with monochromatic Mo–K_α radiation source ($\lambda = 0.71073$ Å). N_{total} reflections were acquired, reducing to N unique (R_{int} quoted) using the proprietary software SMART/SAINT/SADABS/XPREP incorporating 'empirical' absorption corrections, N_o of these with $F > 4\sigma(F)$ being used in the full-matrix least-squares refinements. Anisotropic thermal parameters were refined for the non-hydrogen atoms, $(x, y, z, U_{iso})_H$ being included constrained at estimated values. Conventional residuals on $|F|$, R, R_w (statistical weights) are quoted at convergence. Neutral atom complex scattering factors were employed, computation using the XTAL 3.4 program system [18].

5. Supplementary material

Crystallographic data for the structural analysis have been deposited with the Cambridge Crystallographic Data Centre, CCDC nos. 133432 and 133433 for **3a** and **3b**, respectively. Copies of this information may be obtained free of charge from: The Director, CCDC, 12 Union Road, Cambridge CB2 1EZ, UK (fax: +44-1223-336033 or e-mail: deposit@ccdc.cam.ac.uk or http://www.ccdc.cam.ac.uk).

Acknowledgements

We thank the Australian Research Council and the Special Research Center for Materials and Minerals Processing, UWA, for supporting this work. J.P.H. is the holder of a Materials Institute of Western Australia scholarship. We thank Dr Allan McKinley and his group for use of a high vacuum line.

References

[1] L. Byrne, J.P. Hos, G.A. Koutsantonis, B.W. Skelton, A.H. White, J. Organomet. Chem. (1999) in press.
[2] L.T. Byrne, C.S. Griffith, J.P. Hos, G.A. Koutsantonis, B.W. Skelton, A.H. White, J. Organomet. Chem. 565 (1998) 259.
[3] L.T. Byrne, C.S. Griffith, G.A. Koutsantonis, B.W. Skelton, A.H. White, J. Chem. Soc. Dalton Trans. (1998) 1575.
[4] C.S. Griffith, G.A. Koutsantonis, B.W. Skelton, A.H. White, Chem. Commun. (1998) 1805.
[5] G.A. Koutsantonis, J.P. Selegue, J. Am. Chem. Soc. 113 (1991) 2316.
[6] G.A. Koutsantonis, J.P. Selegue, J.-G. Wang, Organometallics 11 (1992) 2704.
[7] D.W. Shriver, H.D. Kaesz, R.D. Adams, The Chemistry of Metal Cluster Complexes, VCH, Los Angeles, CA, 1990.
[8] M.P. Cifuentes, M.G. Humphrey, in: M.I. Bruce (Ed.), Comprehensive Organometallic Chemistry, vol. 7, Pergamon, Oxford, 1995, p. 907.
[9] P.R. Raithby, M.J. Rosales, Adv. Inorg. Chem. Radiochem. 29 (1986) 169.
[10] M.I. Bruce, Coord. Chem. Rev. 166 (1997) 91.
[11] B.F.G. Johnson, J. Lewis, M.V. Twigg, J. Organomet. Chem. 67 (1974) C75.
[12] E. Lindner, H. Kuhbauch, H.A. Mayer, Chem. Ber. 127 (1994) 1343.
[13] M. Akita, S. Sugimoto, M. Tanaka, Y. Moro-Oka, J. Am. Chem. Soc. 114 (1992) 7581.
[14] M. Akita, Y. Morooka, Bull. Chem. Soc. Jpn. 68 (1995) 420.
[15] G. Frapper, J.F. Halet, Organometallics 14 (1995) 5044.
[16] J.L. Marshall, Carbon–Carbon and Carbon–Proton Couplings, vol. 2, Verlag Chemie, Deerfield Beach, 1983.
[17] G.A. Foulds, B.F.G. Johnson, J. Lewis, J. Organomet. Chem. 296 (1985) 147.
[18] S.R. Hall, G.S.D. King, J.M. Stewart, The XTAL 3.4 User's Manual, University of Western Australia, Lamb, Perth, 1995.